Research Article Vol. 29, No. 11 / 24 May 2021 / Optics Express 17183
Optics EXPRESS

Stimulated Brillouin scattering mitigation using optimized phase modulation waveforms in high power narrow linewidth Yb-doped fiber amplifiers

YUSUF PANBIHARWALA,[1] ACHAR VASANT HARISH,[2] YUJUN FENG,[2] DEEPA VENKITESH,[1] JOHAN NILSSON,[2] AND BALAJI SRINIVASAN[1,*]

[1]Electrical Engineering Department, Indian Institute of Technology Madras, Chennai, India
[2]Optoelectronics Research Center, University of Southampton, Southampton, United Kingdom
[*]balajis@ee.iitm.ac.in

Abstract: We demonstrate the mitigation of stimulated Brillouin scattering (SBS) in a double-clad single mode Yb-doped optical fiber amplifier through external phase modulation of narrow linewidth laser radiation using optimized periodic waveforms from an arbitrary waveform generator. Such optimized phase modulation waveforms are obtained through a multi-objective Pareto optimization based on a comprehensive model for SBS in high power narrow linewidth fiber amplifiers using Brillouin parameters determined from controlled measurements. The ability of our approach to mitigate SBS is tested experimentally as a function of RMS linewidth of the modulated optical radiation, and we measure an enhancement in SBS threshold with respect to optical linewidth of $\sim 10\ \mathrm{GHz}^{-1}$. Furthermore, we discuss the dependence of the SBS threshold enhancement on key parameters such as the amplifier length and the period of the optimized waveforms. Through simulations we find that waveforms of sufficiently long periods and optimized for a relatively long fiber (10 m) are effective for SBS suppression for shorter fibers as well. We also investigate the effect of increase in the bandwidth and amplitude of the modulation waveform on the SBS threshold enhancement observed at higher optical linewidth.

1. Introduction

Stimulated Brillouin scattering (SBS) has the lowest threshold among all the nonlinearities that inhibit power scaling of optical fiber amplifiers for narrow-linewidth, single-transverse-mode laser radiation [1]. Among the various SBS mitigation measures such as, using a short length of large-core fibers [2], applying distributed strain [3] and/or temperature [4] variation along the fiber length, linewidth broadening of a single-frequency laser radiation through phase modulation has been demonstrated to be one of the most effective approaches. Phase modulation with white noise and pseudo random binary sequence (PRBS), normally in the form of a maximum length sequence (MLS), have been studied experimentally and through modeling and simulations in passive as well as active fibers [5–7]. The details of the phase modulation waveforms become quite important to achieve good SBS mitigation. Unfortunately, though the linewidth broadening suppresses SBS, it often degrades the system in other regards (e.g., the combination efficiency of coherently combined systems [8]) and should therefore not be larger than necessary.

For sufficiently long optical fibers ($\sim$ 100 m), noise modulation is reported to provide SBS threshold enhancement close to the theoretical limit for appropriate choices of modulation parameters [5,6]. Here, the enhancement is evaluated from the optical power spectrum, whereas the spectral phase is not important. As such, we refer to this theoretical limit as the "incoherent limit". For shorter fibers, as in the case of an optical amplifier where the length is typically

#425159 https://doi.org/10.1364/OE.425159
Journal © 2021 Received 17 Mar 2021; revised 7 May 2021; accepted 10 May 2021; published 19 May 2021

Optics EXPRESS

in the range of 5 to 10 m, the enhancement in SBS threshold is reported to drop significantly from the incoherent limit [5–7]. We note that these lengths are comparable with the spatial beat period (L_B) for light within the Brillouin linewidth ($\Delta\nu_B = \Gamma_B/2\pi$) [6]. For example, a Brillouin linewidth of 45 MHz would correspond to spatial beat period of $L_B = c/(n_{eff} \times \Delta\nu_B) = 4.6$ m. This drop is especially awkward when a short fiber is used to mitigate SBS. A similar drop in the enhancement efficiency has been reported for other formats such as PRBS, which is found to achieve slightly better results than noise modulation [5,9].

Although noise and PRBS modulation are straightforward to implement with off-the-shelf components, other waveforms may well allow for better SBS suppression. This has motivated further work on numerical optimization or guided by intuition and understanding of SBS. One approach is to target modulation waveforms that result in a nearly rectangular optical spectrum, whether discrete or continuous. This can be achieved through phase modulation with a sum of sines [10], a numerically optimized waveform realized by an arbitrary waveform generator (AWG) [11], or a parabolic function (corresponding to a linear chirp) [12]. In simulations of 9 m of passive fiber, phase modulation with a parabola was found to be better than noise and PRBS modulation, although the required large phase modulation amplitude may be difficult to realize in practice [12]. In experiments, waveforms numerically optimized to achieve rectangular spectra showed some advantage over MLS waveforms for spectral line spacing larger than the Brillouin linewidth [13]. However, their performance became comparable to MLS for smaller spectral line spacings, which are comparable to or smaller than the Brillouin linewidth (e.g., ~ 45 MHz). Such line spacings are small enough for SBS cross-interactions and thus the spectral phase to be significant. Then, it becomes less clear if a rectangular optical spectrum should be preferred.

Another important aspect is that the scope for waveform optimization and the corresponding spectra that can be achieved for PRBS as well as noise modulation are heavily restricted by the small number of optimization variables. This has motivated work on numerical optimization with a much larger number of optimization variables. Such numerical optimization was previously carried out for passive fibers, wherein the Brillouin Stokes power vs. RMS linewidth tradeoff was optimized in the Pareto sense [14]. This means that no other waveforms were found for which the Pareto-objectives (e.g., the Stokes power and linewidth in this case) were simultaneously better. The optimization used a large number of variables (e.g., 40), corresponding to the equidistant sample points on a modulation waveform, which is strictly bandwidth-limited according to the Nyquist-Shannon sampling theorem. In simulations, such sample-optimized waveforms, where the amplitude of the sample points are optimized, produced significantly better results than that obtained using white-noise modulation. Another notable result in this study was that despite cross-interactions, the SBS suppression improved for smaller line-spacings down to 12.5 MHz, which was the smallest considered. The improvement at such narrow line-spacings seems to depend on the spectral phase, although this was not investigated. However, compared to long fibers and the incoherent limit, the enhancement for the shorter fiber lengths of primary interest for amplifiers remained worse than for longer fibers. Furthermore, except for our brief conference report [15], numerical optimization with a large number of variables has not been investigated in amplifiers. For such optimization, the amplifier gain must also be modeled accurately since it contributes to the Brillouin Stokes power and leads to an effective length that is even shorter than the physical fiber length.

In this paper, we demonstrate the generation of sample-optimized periodic waveforms and their utility in mitigating SBS in high power narrow linewidth Yb-doped fiber amplifiers. To achieve this, we extend the model used in [5] to include the gain induced by the Yb-ions and use Pareto-optimization to find the maximum signal output power for different optical linewidths and relative Stokes powers through simulations. The simulations use Brillouin parameters that we determine experimentally. We demonstrate SBS mitigation with optimized waveforms and compare the performance with that predicted by our simulations as well as with similar mitigation

Optics EXPRESS

using noise modulation. Experimentally, the optimized waveforms lead to better SBS threshold than with noise modulation. However, it is worse than in simulations, which we attribute in part to imperfect reproduction of the phase modulation waveform. We further investigate the robustness of optimized waveforms to perturbations or phase errors in the modulated waveform. In addition, through simulations, we investigate the dependence on fiber length, and find that even with optimized phase modulation in amplifiers, the enhancement factor degrades significantly for short fibers. On the other hand, waveforms of sufficiently long periods and optimized for long fiber are found to be as effective as those optimized for short fibers. Finally, we investigate the effect of a restricted modulation bandwidth (determined by the sampling frequency) and amplitude on the optimization. When the amplitude limit of the optimization samples increases from a range of $2\pi(\pm\pi)$ to $4\pi(\pm 2\pi)$, the tradeoff between Stokes power and linewidth improves in some cases, so the Stokes power decreases for some optical linewidths. Improvements are also achieved by increasing the sampling frequency from 600 MHz to 1200 MHz for a constant amplitude of 2π.

2. Modeling SBS in a fiber amplifier

As discussed in the previous section, accurate modeling of our experimental setup is necessary to obtain optimized phase modulation waveforms. In this section, we briefly describe our experimental setup and its simulation model. A schematic diagram of the experimental setup used for studying the mitigation of SBS in a Yb-doped fiber amplifier is shown in Fig. 1. It comprises a 10 m long 5/130 μm (core/clad diameter) ytterbium (Yb)-doped polarization maintaining double clad fiber (Nufern PM-YDF-5/130-VIII) and is pumped at 915 nm. The pump absorption is estimated to be 0.52 dB/m based on fitting simulations to experimental measurements of pump leakage. This value agrees with the manufacturer's specification of 0.6±0.1 dB/m. Thus there is about 5.2 dB total pump absorption across the amplifier length. The length chosen for our work is 10 m as it gives acceptable pump absorption and also falls in the regime where a drop in the SBS threshold enhancement from the incoherent limit is reported. A DFB laser generates narrow linewidth (~100 kHz) light at 1064 nm, which is amplified to about 0.2 W by a pre-amplifier, whose output is used to seed the power amplifier. A lithium niobate phase modulator driven by a radio-frequency (RF) source is placed between the DFB laser and pre-amplifier to broaden the linewidth of the signal by applying the desired modulation waveforms. The power amplifier setup uses free-space components as we want to avoid SBS contributions from any passive fiber in an all-fiber setup. A polarization beam splitter (PBS) at the input end of isolator is used to measure the backward propagating Brillouin Stokes power. We measured the SBS threshold for the power amplifier to be about 2.9 W of output signal power for the case of un-modulated seed laser.

Next, we proceed with the discussion of numerical model for the high power amplifier. A complete time dynamic model for passive optical fibers has been reported in [5,16]. Zeringue et al. [5] have used the model to investigate SBS suppression with phase modulation in a passive fiber. We use equations similar to [5] to describe the SBS and add gain terms to account for the amplification by Yb-ions [17]. Modeling of SBS in the presence of amplifier gain has also been reported in the literature [18–21].

Our model captures the propagation of four waves in an Yb-doped double clad fiber of length (L) 10 m. As per the experimental setup, the amplifier is co-pumped, so the pump ($\lambda_p \sim$ 915 nm) and signal ($\lambda_s \sim$ 1064 nm) are propagating in the forward direction. The Brillouin Stokes at wavelength λ_b (downshifted from signal by a corresponding frequency of ~16 GHz) is propagating in the backward direction and the acoustic wave that couples the signal and Brillouin Stokes wave is propagating in the forward direction. The Brillouin Stokes wave builds up from spontaneous Brillouin scattering due to thermal density fluctuations (modelled as Langevin noise). The Stokes wave beats with the forward propagating signal to generate a forward propagating acoustic wave through electrostriction. This forward propagating acoustic wave enhances the

Optics EXPRESS

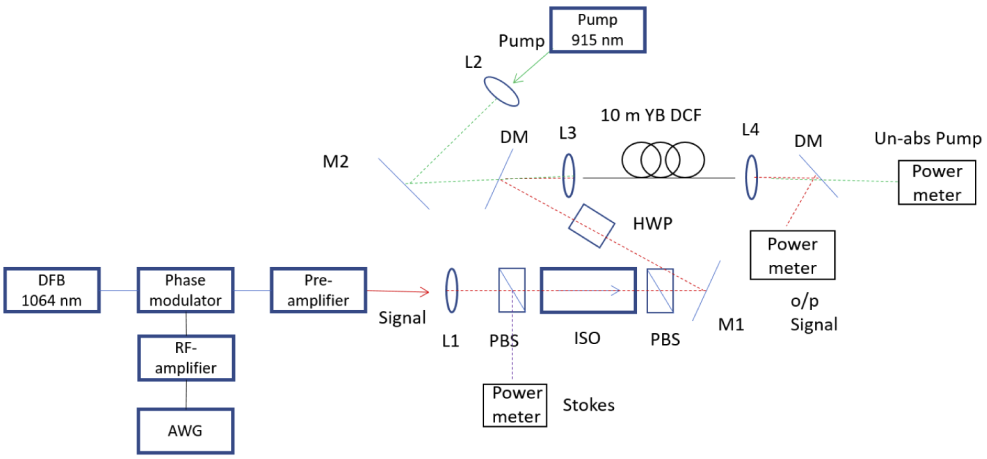

Fig. 1. Experimental setup to test the performance of optimized waveforms for suppression of SBS; DFB: distributed feedback laser, PM: power meter, PBS: polarization beam splitter, ISO: Isolator, M: mirror, L:lens, DM: dichroic mirror, HWP: half wave plate, AWG: arbitary waveform generator.

scattering, leading to SBS. The signal and Stokes waves are assumed to be linearly polarized with the same orientation and hence we use scalar waves in our simulation. The acoustic wave is assumed to be a purely longitudinal pressure wave represented by a variation in the density of the medium (ρ).

The coupled partial differential equations that describe the entire system and models Lorentzian Brillouin gain spectrum are described as follows. The spatio-temporal evolution of the electric field (E_p) corresponding to the amplifier pump wave, which only interacts through the Yb-ions, can be written as [17]:

$$\frac{\partial E_p}{\partial z} + \frac{n}{c}\frac{\partial E_p}{\partial t} = \frac{1}{2}\eta_p[\sigma_{ep}N_2 - \sigma_{ap}N_1]E_p. \tag{1}$$

The evolution of electric fields corresponding to signal (E_s) and Stokes (E_b) are additionally influenced by Brillouin coupling and can be written as:

$$\frac{\partial E_s}{\partial z} + \frac{n}{c}\frac{\partial E_s}{\partial t} = \frac{1}{2}\eta_s[\sigma_{es}N_2 - \sigma_{as}N_1]E_s + i\frac{\gamma_e\omega_s}{2\rho_0 nc}E_b\rho. \tag{2}$$

$$-\frac{\partial E_b}{\partial z} + \frac{n}{c}\frac{\partial E_b}{\partial t} = \frac{1}{2}\eta_s[\sigma_{es}N_2 - \sigma_{as}N_1]E_b + i\frac{\gamma_e\omega_s}{2\rho_0 nc}E_s\rho^*. \tag{3}$$

The evolution of the density of the acoustic wave is given by:

$$2i\Omega_B\frac{\partial\rho}{\partial t} - i\Omega_B\Gamma_B\rho = \epsilon_0\gamma_e k_\rho^2 E_s E_b^* - 2i\Omega_B f. \tag{4}$$

The rate of change of population density of the upper state of Yb-ions (N_2) is given by the following equation:

$$\frac{\mathrm{d}N_2}{\mathrm{d}t} = \frac{\lambda_p\eta_p}{hcA}[\sigma_{ap}N_1 - \sigma_{ep}N_2]P_p + \frac{\lambda_s\eta_s}{hcA}[\sigma_{as}N_1 - \sigma_{es}N_2]P_s + \frac{\lambda_b\eta_s}{hcA}[\sigma_{ab}N_1 - \sigma_{eb}N_2]P_b. \tag{5}$$

where η_p and η_s are the overlap factors with the fiber core for pump and signal respectively. σ_{ep}, σ_{ap}, σ_{es} and σ_{as} are the emission and absorption cross-sections at pump and signal wavelength

Optics EXPRESS

respectively. As the frequency of the signal and Brillouin Stokes wave are close to each other, we consider the same overlap factor as well as absorption and emission cross-section for Stokes and signal waves. N_1 and N_2 are the population densities of the lower and upper levels of the Yb-ions, γ_e is the electrostrictive constant, c is the speed of light in free space and n is the refractive index of the medium, f is the Langevin noise source in the medium, that models the thermal excitation of acoustic waves, which in turn initiates the SBS process, Γ_B represents the Brillouin gain bandwidth in angular frequency, Ω_B is the resonant acoustic angular frequency of the medium, k_ρ represents the wavenumber of the acoustic wave, h is the Planck's constant and A is the core area of the optical fiber.

We introduce phase modulation of the signal wave through the boundary conditions $E_s(z = 0, t) = E_s^{in} e^{i\phi(t)}$, where E_s^{in} denotes the amplitude of the input signal field which is a constant and $\phi(t)$ denotes the phase modulation waveform. Here $\phi(t) = \pi V(t)/V_\pi$, where $V(t)$ is the instantaneous voltage of the RF wave applied to drive the phase modulator and V_π is the voltage at which the phase modulator provides π phase change. The inherent phase noise due to the linewidth of the laser (~100 kHz) is assumed negligible compared to optical linewidth achieved after phase modulation. For the Brillouin Stokes wave, the initial and boundary conditions are given by $E_b(z, t = 0) = E_b(z = L, t) = 0$ [5]. Initial and boundary conditions for the acoustic wave become $\rho(z = 0, t) = \rho'_{(0,k)}$ and $\rho(z, t = 0) = \rho'_{(j,0)}$, where ρ' is given by [5]:

$$\rho'_{(j,k)} = \sqrt{\frac{nQ}{c\Gamma_B}} S_{(j,k)}. \tag{6}$$

Here $S_{(j,k)}$ is a complex Gaussian random variable with zero mean and unit variance. j and k represent discrete variables along length (z) and time (t) respectively. Q is given by $2\Gamma_B k T \rho_0 / v_s^2 A_{eff}$, where A_{eff} is effective interaction area [5]. Similarly, the Langevin noise term is defined as:

$$f_{(j,k)} = \sqrt{\frac{nQ}{\Delta t^2 c}} S_{(j,k)}. \tag{7}$$

The initial condition for upper state Yb-ions (N_2) is obtained by solving Eqs. (1), (2), and (5) for the steady state of the Yb-amplifier (i.e. making $\frac{\partial}{\partial t} = 0$ and considering only the presence of pump and signal at the input of the amplifier and neglecting Brillouin Stokes generation). This calculation of the initial condition for N_2 helps in reducing evaluation time and thus the Stokes evolution in the amplifier can be calculated in a similar time-scale as in passive fiber. Equations (1)–(5) are then numerically solved using a modified Euler technique similar to [5]. For a CW input signal, the Brillouin Stokes power still fluctuates in time. To calculate the average Stokes power we evaluate the instantaneous Stokes power for at least 20 transit times, corresponding to signal propagation through the fiber length in our simulations and discard the initial two transits, which correspond to the Stokes buildup time. We define the SBS threshold as the output signal power corresponding to a relative Stokes power value of 0.01 [5], where the relative Stokes power is defined as the ratio of average backward Stokes power to amplified output signal power. We note that SBS can lead to pulses with high energy [22] which may well modulate the Yb-gain. However, at 1% of relative Stokes power, the average Stoke power as well as the energy in any pulses are expected to have a negligible effect on the Yb gain. Thus, we can neglect SBS when calculating the Yb gain.

In order to emulate the experiment accurately, we need to determine certain parameters, notably the Brillouin gain bandwidth (Γ_B) and electro-strictive constant (γ_e) for our fiber. These parameters are determined by matching simulations to experiments, performed with a signal broadened by sinusoidal phase modulation of amplitude $\pm\pi$. The threshold for an un-modulated signal is largely determined by the value of Brillouin peak gain (g_B), which is directly proportional to γ_e^2 and inversely proportional to Γ_B [16]. We simulated multiple combinations of Γ_B and γ_e, which result in similar values of g_B and SBS threshold as in the experiments with an un-modulated

Optics EXPRESS

signal. Figure 2 shows the SBS threshold measured through experiments, and that through simulations for different sinusoidal modulation frequencies. We observe that the SBS threshold in simulation obtained for $\Gamma_B = 2\pi \times 45 \times 10^6$ rad/s and $\gamma_e = 1.2$, is closer to the experimental results across various modulation frequencies as shown in Fig. 2. Thus, we choose to use these values of Γ_B and γ_e in our simulation model to obtain optimized modulation waveforms. Furthermore, Γ_B is equal to the inverse of the lifetime of the phonons of the acoustic wave, which thus becomes

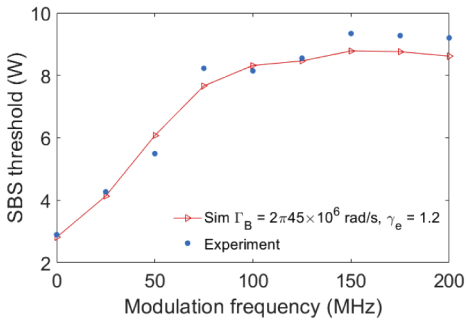

Fig. 2. Comparison between simulated and experimentally obtained values of the SBS threshold achieved using phase modulation with sine waveform for various values of modulation frequency.

Table 1. The key parameters in our model and the corresponding values considered in our simulations.

Quantity	Symbol	Value	Comments
Electrostrictive constant	γ_e	1.2	obtained from our experiments by comparisons with simulations
Background density of fiber	ρ_0	2201 kg/m^3	taken from [5]
Resonant acoustic angular frequency of the medium	Ω_B	$2\pi \times 16 \times 10^9$ rad/s= 10.1×10^{10} rad/s	taken from [5]
Brillouin gain angular bandwidth	Γ_B	$2\pi \times 45 \times 10^6$ rad/s = 283×10^6 rad/s	obtained from our experiments by comparisons with simulations
Overlap factor for pump, signal	η_p, η_s	0.0015, 0.6241	calculated from Yb-doped fiber parameters
Emission, absorption cross-section at pump wavelength	σ_{ep}, σ_{ap}	$0.0193\times10^{-24} m^2$, $0.5693\times10^{-24} m^2$	provided by fiber manufacturer
Emission, absorption cross-section at signal wavelength	σ_{es}, σ_{as}	$0.3978\times10^{-24} m^2$, $0.0064\times10^{-24} m^2$	provided by fiber manufacturer
Yb-ions concentration	N	1.42×10^{26} m^{-3}	N=clad absorption/($\sigma_{ap}\eta_p$), where clad absorption is determined as 0.52 dB/m at pump wavelength
Core area	A	19.6 μm^2	provided by fiber manufacturer
Maximum and minimum phase limit for modulation waveform	ϕ_{min}, ϕ_{max}	$-\pi, \pi$	user defined limit for Pareto variables

Optics EXPRESS

$(2\pi \times 45 \times 10^6$ rad/s$)^{-1}$ = 3.5 ns (here and throughout this paper, we assume that the Brillouin line is Lorentzian and homogeneously broadened). The parameters and their values used in simulations are shown in Table 1.

3. Multi-objective Pareto-optimization for finding phase modulation waveforms

As mentioned in the Introduction, we use the above model for determining the "optimized" waveform for external phase modulation of the seed laser. In our work, a multi-objective Pareto optimization returns the best trade-off (i.e., the "Pareto front") it finds among multiple simultaneous objectives. In case of SBS mitigation in optical fibers, the objectives of high threshold and narrow linewidth are both desirable, but there is a well-known tradeoff between them. Pareto optimization finds the phase modulation waveforms that represent the best options for the trade-off, in the sense that no other waveforms were found that are better in both threshold and linewidth compared to any of the waveforms in the Pareto-optimized set [23].

Although the concept is simple, there are many practical difficulties. During the optimization, there will be waveforms with significantly lower or higher relative Stokes power. For example, the solution obtained with lower relative Stokes power which usually occur at larger linewidths may be dominated by spontaneous Brillouin scattering. This is a linear effect which cannot be used for optimization. Furthermore, the results obtained with very high relative Stokes power typically contain numerical errors [5]. To overcome these issues, we varied the amplifier pump power according to the linewidth and also bound the relative Stokes power to be within 0.03 to 0.2. To implement this, we choose three Pareto objectives to be optimized simultaneously. The three objectives are the RMS linewidth of the input signal optical spectrum [14], the relative Stokes power, and the output signal power. Also, we make the amplifier pump power a variable along with the equidistant points (samples) to be optimized for the waveform.

As shown in Fig. 3, the Pareto optimization procedure is initiated with 'n' arbitrary sample values of phase chosen between ϕ_{min} and ϕ_{max}. These phase values are passed on to the theoretical amplifier model along with the pump power to determine the relative Stokes power, the output signal power, and the linewidth of the optical spectrum. Such parameters are optimized using the Pareto Toolbox, thereby yielding the phase values of the optimized waveform. The waveform is periodic and equidistantly sampled, but we consider different periods including those that are longer than all time constants in the SBS process, i.e., the phonon lifetime and the fiber's roundtrip propagation time. The optimizer varies the pump power as the linewidth varies such that the relative Stokes power falls within the above bound with maximum signal power at the output. Thus, instead of the conventional approach of a pre-defined relative Stokes power for which the maximum signal power is found versus linewidth, this will provide optimized triplets of linewidth (smaller is better), relative Stokes power (smaller is better), and signal output power (larger is better) for a system designer to choose from. A lower pump power is clearly better, too, if it equates to higher efficiency, but the pump power is expected to follow closely from the pump absorption (which is nearly constant, since the fiber length is fixed) and the signal output power.

For the multi-objective optimization, we use a genetic algorithm from the optimization toolbox in MATLAB. We first consider phase modulation waveforms with 12 MHz repetition frequency and 50 points (n) to be optimized along the waveform, corresponding to a sampling rate of 12 MHz ×50= 600 MHz. As described above, the amplifier pump power is made a variable for optimizer together with the amplitude of the waveform. For our initial simulations, the amplitude of the waveform points to be optimized is given a lower and upper bound of $-\pi$ and $+\pi$ radians respectively. Similarly a lower and upper bound is provided for the pump power based on our initial guess values of lowest and highest pump power required by the amplifier algorithm to provide relative Stokes power within the given bound of 0.03 to 0.2 for signals with modulation. The simulation model described in the previous section is used to calculate the values of the three optimization objectives (RMS linewidth , output signal power and relative Stokes power)

Optics EXPRESS

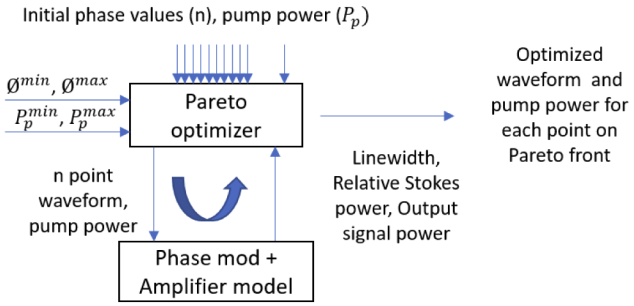

Fig. 3. Schematic representation of our approach to determine optimized phase modulation waveforms with the help of a comprehensive model of the fiber amplifier.

for a particular set of waveform optimization points (ϕ_n) and pump power. For the simulations, we resample the modulation waveform to a higher sampling rate of $1/\Delta t$ (≈10 GHz), where $1/\Delta t$ corresponds to the discrete time sampling step considered in simulations. For resampling we evaluate a sum of weighted and time delayed sinc functions as mentioned in [14]. This is a standard approach, and the sinc-functions have a maximum bandwidth of half the rate of the optimized points. However, phase modulation as well as SBS are nonlinear processes, so the signal and Stokes waves will generally not be bandwidth-limited (which is why denser resampling is necessary). Note also that resampled points can overshoot the optimized points. The overshoot scales with the logarithm of the number of samples. Thus, in theory it can be infinite with an infinite number of optimized points, but was generally less than 10 percent in our simulations (shown in Fig. 4(b)).

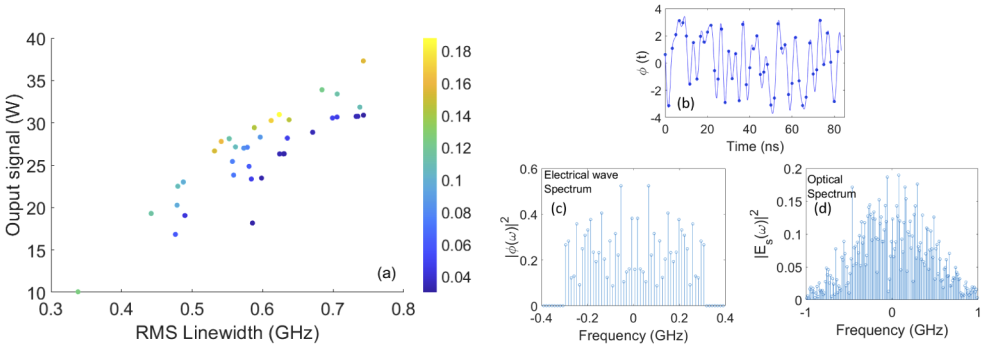

Fig. 4. (a)The trade-off between three optimized objectives (Pareto front) as obtained for a 10 m long Yb-doped fiber amplifier, where each point represents the performance of an optimized waveform. The colour bar on the right side represents relative Stokes power. (b) Time trace for one of the optimized waveforms with 650 MHz optical linewidth (RMS), where the blue dots represent the 50 points obtained through the optimization and blue trace shows the re-sampled waveform, (c) the corresponding electrical waveform PSD ($|\phi(\omega)|^2$) and (d) optical signal spectrum obtained after phase modulation as downshifted to the baseband ($|E_s(\omega)|^2$).

Figure 4(a) shows the results of the Pareto optimization in terms of the three optimization objectives. The color represents the third objective, i.e., relative Stokes power. For each optimized triplet of objectives, we obtain the corresponding 50 optimized phase modulation points and amplifier pump power. As seen from Fig. 4(a), our optimization routine has yielded multiple waveforms corresponding to different values of the relative Stokes power, output signal power

Optics EXPRESS

and signal linewidth. In Fig. 4(b) we show one such optimized waveform, where the blue dots represent the 50 optimized phase points (ϕ_n) and the blue curve represents the waveform resampled at 10 GHz . The power spectral density (PSD) of the modulation waveform and the corresponding phase-modulated optical signal spectrum are also plotted in Figs. 4(c) and 4(d) respectively. This confirms that the modulation waveform spectrum extends to half of the 600-MHz rate of the optimized points, so the double-sided width becomes 600 MHz. The optical spectrum extends further than shown in Fig. 4(d), but is still well-contained in the range ± 1 GHz.

The optimized data can be further analyzed to obtain the SBS threshold power as a function of signal linewidth. For each optimized waveform, we calculate the SBS threshold power, i.e., the output signal power corresponding to a relative Stokes power value of 0.01. Note that except when the relative Stokes power is close to 0.01 for a triplet in the Pareto-optimization, these waveforms are not optimized for the highest SBS threshold power (as defined in that way). However, they are generally expected to come close to achieving the optimized threshold. The SBS threshold calculated for each optimized waveform is plotted in Fig. 5. For similar linewidths, there are several optimized waveforms obtained with different relative Stokes power and their SBS thresholds are close to each other.

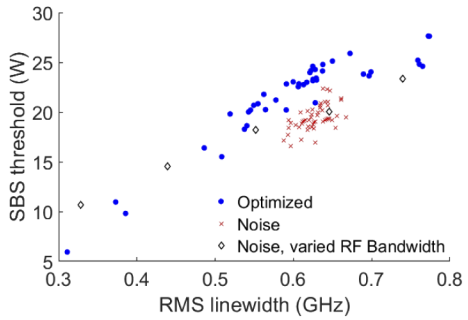

Fig. 5. SBS threshold obtained for each optimized waveform shown in Fig. 4(a) compared with SBS threshold for 50 noise modulation waveforms.

3.1. Comparison with noise modulation

Next, the performance of optimized waveforms is compared to that of noise modulation. A first set of noise modulation waveforms are made from uniformly distributed uncorrelated random numbers between -π and +π with the sampling rate of 600 MHz as for the optimized waveform. The length of the noise modulation waveform is equal to the total simulation time considered for optimized waveforms (i.e., the time of 20 transits through the length of the fiber). We simulated over 50 such noise waveforms. This is also equivalent to running a simulation for a single noise waveform for the time of 20×50 transits, measuring the threshold and RMS linewidth in each interval corresponding to the time taken for 20 transits across the fiber amplifier. The performance of noise waveforms is plotted in Fig. 5 (red cross points). We observe that this set of noise waveforms results in optical linewidths in the range of 0.6-0.66 GHz and SBS thresholds in the range 17-22 W. This significant fluctuation in SBS threshold even though the noise statistics are the same and the linewidths are similar highlights one of the drawbacks of noise modulation compared to any fixed format phase modulation, i.e., the noise modulation provides a larger level of uncertainty in the SBS mitigation. In addition, we observe that our optimized waveforms outperform this set of noise waveforms as illustrated in Fig. 5. To quantify the improvement, we consider the mean value of the linewidth and the lowest value of the SBS threshold for noise waveforms. The lowest value of the threshold for noise is considered because we expect a system designer would have to stay well below the corresponding SBS threshold power to remain in a

Optics EXPRESS

safe operating regime. Tracking this regime is important, since it has been reported that higher relative Stokes power can result in Stokes pulses with high peak power from the fiber amplifier, which may destroy the amplifier as well as the pump lasers [22]. A comparison of limits for potentially destructive pulsing between optimized and noise modulation is interesting but outside the scope of this paper. The mean linewidth for noise is 0.63 GHz and the lowest threshold is 16.9 W. Optimized waveforms with 0.63 GHz linewidth show SBS thresholds of 24.6 W. Thus, the SBS threshold power achieved for optimized waves is around 1.45 times as high as noise modulation in this case. Although that is relative to the lower value (16.9 W) with noise modulation, the optimized waveforms are also around 1.26 times the average noise-modulation value.

We next evaluate noise modulation performance for different optical linewidths. For this we generate noise waveform in a similar manner as described above with random samples at 600 MHz and additionally pass the waveform through a low pass filter and an RF amplifier before feeding it to the phase modulator [5,6]. The low pass filter bandwidth is varied to achieve different optical linewidths and the RF amplifier gain is set to scale the amplitude of waveform within the range $\pm 2\pi$. We evaluate the SBS threshold for 10 such waveforms at each optical linewidth we consider and plot the average performance in Fig. 5 (Black diamonds). We observe that the average noise performance obtained earlier by 50 waveforms with amplitude range $\pm\pi$ is close to the average performance obtained by 10 low-pass filtered waveforms with amplitude range $\pm 2\pi$ near 650 MHz RMS linewidth. Furthermore, when comparing optimized waveform performance with the noise performance obtained at various optical linewidths, we note that the performance of optimized waveforms rolls off beyond the range of linewidths obtained with 50 noise modulation waveforms. This issue can be solved if we relax the limits imposed on modulation bandwidth and amplitude while performing the Pareto optimization, as will be shown in the Discussion section.

3.2. Effect of varying waveform's period

To study the effect of period of the waveforms, we carried out Pareto optimization with the same three objectives for different waveform repetition frequencies, 6, 24 and 50 MHz (in addition to 12 MHz). The sampling rate of the optimized points is kept constant at 600 MHz, so that the optical linewidths that can be achieved are similar in all four cases. This means that the number of waveform points to optimize varies, and reaches 100 points at 6 MHz waveform repetition frequency. SBS thresholds achieved for optimized waveforms are plotted in Fig. 6. The trend looks similar for all the above waveform repetition frequencies with a slight improvement in threshold as the repetition frequency is reduced (most evident for linewidths around 0.65 GHz). This trend may be understood as follows: If we consider a modulated waveform with a repetition frequency of 12 MHz (period 83.3 ns), this corresponds to a spatial range of 17.1 m which covers 8.6 m of fiber roundtrip propagation (given that signal and Stokes are counter-propagating). With our 10 m fiber length, this allows nearly all light that has been modulated by the waveform in one period and back-scattered through SBS to exit the fiber before the end of that period. With a shorter period (e.g., for 24 MHz), the lightwaves in the fiber have a "memory" from one period of the modulation waveform to the next, which restricts the optimization. This also means that in principle, waveforms with 6 MHz waveform repetition frequency cannot be worse than the 12 MHz case. However, in practice they may appear to be, if the large number of sampling points to optimize for 6 MHz waveform impairs their optimization. Thus, we observe that for a given amplifier length the optimum length of the periodic waveform is somewhere close to the spatial length corresponding to the roundtrip time. This is further discussed in detail in the Discussion section. We note also that the phonon lifetime of 3.5 ns is short compared to the roundtrip propagation time as well as the lengths of the modulation waveforms.

Optics EXPRESS

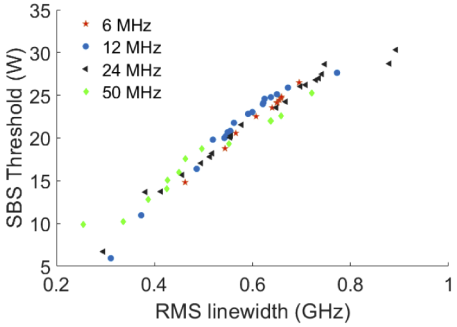

Fig. 6. SBS threshold calculated for optimized waveforms obtained at various repetition frequency for a 10 m amplifier length

4. Experimental results

The simulation results presented above exhibit a high level of promise for the use of optimized waveforms to mitigate SBS in high power narrow linewidth fiber amplifiers. Such results need to be validated with controlled experiments, which are described here. We use an arbitrary waveform generator (AWG) with 12 GHz sampling frequency to generate the optimized waveforms. For this, the optimized waveform is resampled at 12 GHz using a similar procedure as used in simulations and fed to the AWG. The high resampling rate can improve the fidelity of the waveform generated by the AWG, which is otherwise expected to deviate from the ideal recreation as a sum of sinc functions with bandwidth equal to half of the sampling frequency e.g., as a result of non-ideal filtering. A combination of a RF amplifier at fixed gain and a variable RF attenuator is used to adjust the RF drive power of the phase modulator, to achieve the desired modulation amplitude. The RF amplifier has a 3-dB bandwidth of 700 MHz, which is sufficient to support the 300 MHz bandwidth of our resampled waveforms. However, the gain measured for the RF amplifier and attenuator was not constant over this frequency range. Therefore, we modified the AWG samples to correct for this [13], and were thus able to reproduce the waveforms with a maximum error of ~0.2 V, which corresponds to ~0.3 rad ($\phi = \pi V/V_\pi$). The effect of such errors is discussed in detail in the Discussion section.

We measured the SBS threshold power and RMS linewidth for our optimized waveforms obtained for a 10 m amplifier length and a waveform repetition frequency of 12 MHz. For measuring the RMS linewidth, a homodyne method is used where the phase modulated signal is allowed to beat with an unmodulated light on a high speed photo-detector. The output of the photo-detector is recorded on an electrical spectrum analyser. The results are plotted in Fig. 7(a). A SBS threshold of 20 W is measured for a RMS linewidth of 0.68 GHz, which translates to an enhancement factor of about 6.9, where the enhancement factor is obtained by dividing the SBS threshold after modulation with the un-modulated threshold (2.9 W). This enhancement factor of 6.9 achieved at 0.68 GHz RMS linewidth waveform translates to an enhancement slope of 10 GHz^{-1}. An enhancement slope of 7.7 GHz^{-1} is reported with PRBS modulation at an optical linewidth of 1.7 GHz (FWHM) with a similar (Nufern PM-YDF-5/130) fiber and amplifier length [7]. Here, it has to be noted that the linewidth definition used to obtain performance in [7] is FWHM. Thus, the comparison between the two results is not straightforward. PRBS modulation (un-filtered) is reported to result in a $sinc^2$ spectrum, for which we found that the RMS linewidth is 5 % larger than the FWHM linewidth. In such a scenario, the PRBS performance translates to 7.25 GHz^{-1} in terms of RMS linewidth. Thus, the enhancement slope of 10 GHz^{-1} obtained for the optimized waveforms look favorable compared to enhancement slope of 7.25 GHz^{-1} reported for PRBS waveforms. However, as the enhancement factor depends on fiber properties like

Optics EXPRESS

Brillouin peak gain and bandwidth, a simple direct comparison of results obtained in different cases may not be justified. We also note that an enhancement slope of 10.6 GHz^{-1} (FWHM) was reported recently with PRBS modulation with a larger core fiber and shorter amplifier length for < 5 GHz optical linewidth [9]. Back-to-back comparisons with proper optimization may be needed to quantify the improvements possible with waveforms sample-optimized with a minimum of restrictions. We also note that the enhancement slope becomes 17.7 GHz^{-1} with respect to the RMS linewidth of a Gaussian optical spectrum in the incoherent limit. The enhancement slopes for different common spectral shapes and linewidth definitions are presented in Appendix.

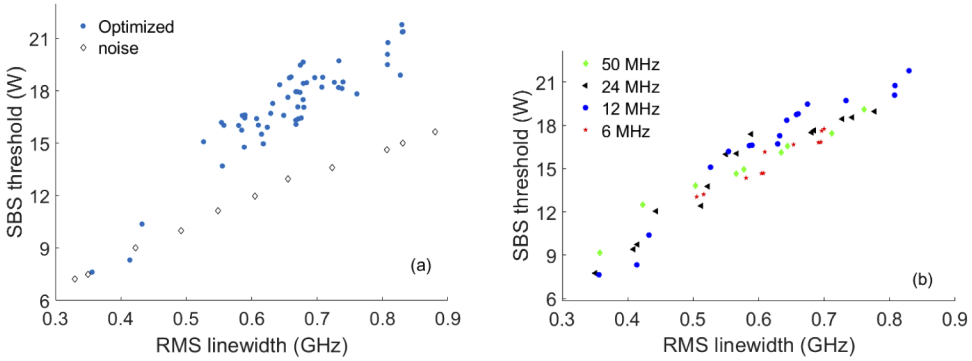

Fig. 7. Experimentally measured SBS threshold for optimized waveforms obtained for an amplifier length 10 m at (a) 12 MHz frequency spacing and compared with noise modulation and (b) various frequency spacings.

We experimentally compared the performance of our optimized waveforms with that of noise modulation. We generated the noise waveform using a uniform random number generator whose output is passed through a low pass filter and the amplitude of the resultant waveform is scaled appropriately in simulations (similar to the method presented in Sec. 3). The noise was generated for a longer 0.7 ms time period. The RF filter bandwidth was varied to achieve different waveforms with different values of optical linewidth. This generated waveform was then fed to the AWG to obtain noise modulated optical signal. The measured SBS threshold is plotted in Fig. 7(a) as a function of linewidth for noise as well as for our optimized waveforms. The enhancement factor measured for noise is 4.5 at 0.65 GHz linewidth, which corresponds to an enhancement slope of 6.92 GHz^{-1}. Thus, we found that experimentally optimized waveform yields an enhancement slope which is about 1.44 times better than for noise modulation, which matches well with the value (1.45 times which is calculated with lowest value of threshold) observed in simulations. We also perform experiments with optimized waveforms obtained for waveform repetition frequencies of 6, 24 and 50 MHz. The results are plotted in Fig. 7(b) which shows a similar trend as observed in the simulation results shown in Fig. 6.

5. Discussion

5.1. Comparison of SBS threshold enhancement in simulation and experiments

The SBS thresholds measured after modulation with optimized waveforms (red points) in the above experiments is lower than that estimated from simulation results (blue points) as seen in Fig. 8(a). We attribute in part this shortfall in experimental suppression to a slight mismatch in the experimental reproduction of optimized waveforms by the AWG, RF amplifier, and/or phase modulator. An experimentally generated optimized waveform with RMS linewidth of 650 MHz

Optics EXPRESS

and 12 MHz repetition frequency is plotted in Fig. 8(b) along with a simulated waveform. The experimental waveform is calculated from the measured voltage fed into the phase modulator.

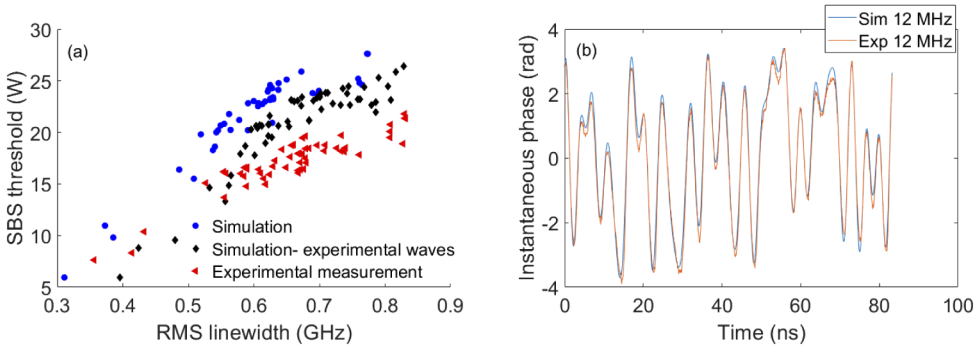

Fig. 8. (a) Simulated SBS thresholds with optimized waveforms (blue) and experimentally measured waveforms (black) plotted along with experimentally measured SBS threshold (red) and (b) time trace of a simulated waveform with optical linewidth of 650 MHz to be generated by AWG (blue) and experimental waveform (as recalculated to phase) fed to the phase modulator (red).

Compared to the simulated waveform, we observe a small error for the experimentally generated waveform. To find the sensitivity of the SBS threshold to this error, we calculate the threshold with simulations run with the experimentally generated waveforms. The SBS threshold obtained for all the waveforms is plotted in Fig. 8(a) (black points). We observe that all the experimental waveforms lead to a simulated threshold that is worse than that of the waveforms optimized in simulations, but better than the threshold measured in experiments. Thus, the non-ideal reproduction of the waveforms appears to partly explain the degradation in experimental SBS suppression. Other factors affecting the results can be uncertainties in the fiber parameters and the overall model (e.g., the assumption of scalar waves) used for the simulations. This would lead to waveforms that are optimized for an amplifier or conditions that differs from the actual case.

5.2. Performance of waveforms optimized for different lengths

The enhancement factor for the SBS threshold by phase modulation is reported to reduce for decreasing length (e.g., below 10 m) in passive fibers for noise and PRBS modulation formats even when details such as clock frequency and RF power (i.e., modulation amplitude) are optimized for a specific length [5,6]. A related question is how well a waveform optimized for a specific amplifier length performs at other lengths. To study this, we simulate amplifiers of different lengths with a modulation waveform optimized for 10 m. We keep the total pump absorption constant at 5.2 dB (the absorption obtained previously for 10 m amplifier length) by changing the pump wavelength to yield a higher absorption per unit length for shorter amplifiers. To limit the change in pump wavelength to a smaller value, we used a wavelength of 971 nm for a length of 10 m. This results in the same absorption as obtained previously with 915 nm pumping. As we reduce the fiber amplifier length, we tune the pump wavelength closer to the absorption peak at around 975 nm. We first choose one optimized waveform obtained with 10 m amplifier length for each value of waveform repetition frequency with linewidth around 650 MHz and compute enhancement factors for lengths varying from 3.5 to 15 m. The simulation results are plotted in Fig. 9(a). Similar to previous results [5], the enhancement factor decreases for shorter amplifiers. We also observe that for the shorter amplifiers, all waveform repetition frequencies perform similarly but for longer amplifiers the longer waveforms (with smaller repetition frequency) perform better. The 20 ns period of the 50 MHz waveform corresponds to

Optics EXPRESS

4.1 m of fiber propagation (2.1 m round-trip), which we believe is a reason why the 50 MHz curve falls off for fibers longer than 4-5 m.

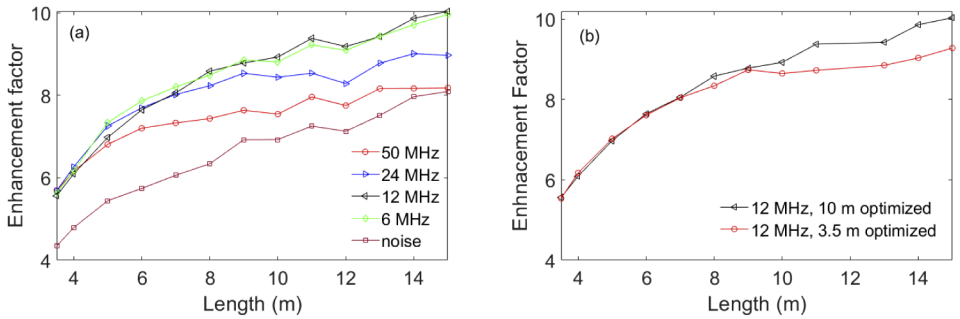

Fig. 9. Length dependence of the enhancement factor achieved for (a) optimized waveforms with 650 MHz linewidth obtained for 10 m amplifier at various frequency spacing and their comparison with noise modulation of similar linewidth and (b) optimized waveforms with 650 MHz linewidth obtained for 10 m and 3.5 m amplifier length at 12 MHz frequency spacing

In addition, we observe that long period waveforms perform well for all investigated fiber lengths. Furthermore, as mentioned earlier, a longer waveform can in theory never be worse than a shorter one (at least if it is longer by an integer factor), so we attribute the absence of performance improvement for 6 MHz waveform compared to 12 MHz waveform to imperfect optimization. In contrast, for long fibers, shorter waveforms are increasingly worse, even when optimized for long fibers. Short waveforms can perform as well as the long ones for short fibers, but in no case did they perform better than the long waveforms. We also performed Pareto-optimization at shorter fiber lengths (i.e., at 3.5 m) with the long period waveform (i.e., 12 MHz) and evaluated its performance across various lengths. We found that for longer fibers, long period waveforms optimized at such lengths (i.e., 10 m in our case) performs slightly better than those optimized for shorter fibers (shown in Fig. 9(b)). On the other hand, in shorter fibers their performance is found similar. Thus, to the extent that computational power and modulation hardware suffice, long waveforms seem best, and even when optimized for long fibers they seem to perform close to optimum also for short fibers.

We also compare the results with the enhancement factors obtained with noise modulation. Here, the noise waveforms are generated as in the previous simulations and the enhancement factor of the SBS threshold is computed for each length based on the average performance of many trials of noise waveforms. As seen from Fig. 9(a), the noise waveforms do not perform as well as the optimized waveforms, except in cases where the optimized waveform period is too short relative to the fiber length.

5.3. Simulation with larger linewidths

We next perform simulations to demonstrate the performance of the optimized waveforms at larger optical linewidths, potentially leading to kW level output power. Larger linewidths can be achieved by increasing the modulation depth (RF power) as well as the sampling frequency (RF bandwidth). Increasing the sampling frequency for a fixed frequency spacing means more points (n) to optimize. On the other hand, the maximum value of modulation depth depends on the available RF power and/or the RF power handling and the V_π-value of the phase modulator being used. We next optimize the 12 MHz waveform with twice the sampling rate of optimized points as previously used (1200 MHz instead of 600 MHz), while maintaining the modulation depth at $\pm\pi$. In addition, we optimize the case with the 600 MHz sampling rate of optimized

Optics EXPRESS

points (as previously) but twice the modulation depth, $\pm 2\pi$. Both of these changes are expected to approximately double the signal linewidth that can be achieved. The SBS thresholds achieved for Pareto-optimized waveforms is plotted in Fig. 10. We observe that the optimized waveform are obtained in the RMS linewidth region between 0.9 GHz to 1.5 GHz. This is because the lower and upper bound provided for the pump power was chosen such that the optimization yields waveforms appropriate for kW-level power-scaling. The mean enhancement slope calculated for larger phase modulation depth i.e., $\pm 2\pi$ with 600 MHz sampling rate is about 12.8 GHz^{-1} which is better than the 11.5 GHz^{-1} mean enhancement observed for $\pm\pi$ with 1200 MHz sampling rate. A possible explanation is that the optimization routine finds it more difficult to find global optima with the large number of points (100) in the 1200 MHz sampling case, but further investigations are needed to confirm this. Also, we observe that the enhancement slope for waveforms obtained with $\pm 2\pi$ modulation depth and 600 MHz sampling rate increases for lower RMS linewidth. We believe that it would atleast match the performance of waveforms obtained with $\pm\pi$ modulation depth and 600 MHz sampling at lower RMS linewidths (below 0.9 GHz), since modulation depth limit of $\pm\pi$ is a subset of $\pm 2\pi$ modulation depth. Please note that the results obtained with $\pm\pi$ modulation depth and 600 MHz sampling, which shows a mean enhancement slope of 13.8 GHz^{-1} are re-plotted from Fig. 5 for comparison. Regardless, we expect that modulation waveforms that allow for larger optical linewidths lead to larger enhancement factors and thus to scaling beyond 1 kW of output power even with relatively small cores.

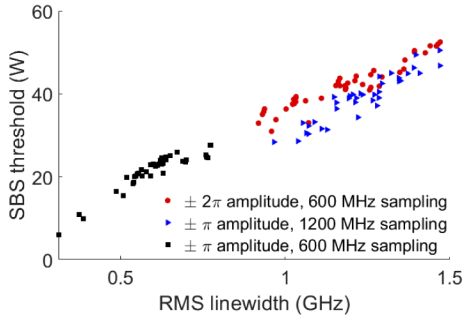

Fig. 10. SBS threshold for optimized waveform obtained with higher sampling rate or modulation depth for a 10 m amplifier length and compared with results obtained with lower sampling rate and lower modulation depth

6. Conclusion

In conclusion, we have demonstrated the mitigation of SBS in Yb-doped fiber amplifier through external phase modulation of a narrow linewidth source using optimized periodic waveforms. To the best of our knowledge, this work constitutes the first demonstration of SBS mitigation with waveforms optimized based on a comprehensive amplifier model including Brillouin parameters extracted from measurements. The optimized waveforms used in our work result from multi-objective Pareto optimization involving the RMS linewidth of the optical signal, output signal power, and relative Stokes power.

In case of a modulation bandwidth limited to 300 MHz and modulation amplitude limited to $\pm\pi$ radians, it was possible to reach an enhancement factor for the SBS threshold relative to that without phase modulation of 6.9 for an optical linewidth of 650 MHz, corresponding to an enhancement slope of ~ 10 GHz^{-1}. Modulation waveforms with relaxed limits on modulation bandwidth and amplitude allowed for larger optical linewidths, and larger SBS thresholds approximately in proportion. An enhancement factor of nearly 15 was reached for RMS linewidth of 1.3 GHz, which is expected to allow for kW-level power scaling in fibers with larger cores than

Optics EXPRESS

we studied. The SBS mitigation is also studied for different lengths of the modulation waveform. In simulations, we found that a modulation waveform optimized for a fiber length of 10 m could be effective for lengths in the range 3.5 – 15 m, corresponding to fiber roundtrip times of 34 – 146 ns, but only if the modulation waveform was sufficiently long. Thus, an 83.3-ns waveform (12 MHz frequency) worked well for this range, whereas a 20 ns waveform (50 MHz frequency) proved worse for fibers longer than 5-6 m.

Experimentally, we verified the increase in SBS threshold in different cases, although it was slightly degraded compared to simulations. We found that experimental waveforms deviations from the simulated waveforms could partly explain this degradation, although imperfections in the model and parameter values are also expected to contribute. Nevertheless, we still found that the optimized waveforms provide 1.4 times higher enhancement in SBS threshold than noise modulation did. The relative enhancement improvement of optimized waveforms agreed with that obtained in simulations.

Appendix A: Impact of lineshape and linewidth metric on incoherent Brillouin gain

Here we consider the peak Brillouin gain in case of a broadened optical spectrum with lineshape $S(\nu)$ in the incoherent approximation for a Lorentzian Brillouin lineshape with FWHM linewidth $\Delta\nu_B$. For simplicity, we consider optical line shapes for which the position of the Brillouin gain peak stays the same. The optical lineshape is normalized so that $\int_{-\infty}^{\infty} S(\nu)d\nu = 1$ and shifted in frequency with peak at frequency $\nu = 0$. The Brillouin profile $g_B(\nu, \nu_0)$ can be written as $g_{B,0}/\{1 + 4[\nu - (\nu_0 - \nu_B)/\Delta\nu_B]^2\}$, where $g_{B,0}$ is the peak value and ν_0 is the optical frequency of the Brillouin pump (i.e. signal) [24,25]. In case of monochromatic Brillouin pump, this directly determines the Brillouin gain at frequency ν, including the peak gain, following scaling with Brillouin pump intensity and fiber length. Without loss of generality, we will assume these equal to unity.

In the more general case of a broadened Brillouin pump, different parts of the pump spectrum contribute to the Brillouin gain $G_B(\nu)$ at frequency ν according to the value of $g_B(\nu, \nu_0)$. This can be evaluated as a convolution (represented by *) of the Brillouin pump spectrum and the Brillouin lineshape:

$$G_B(\nu) = g_B(\nu, \nu_0) * S(\nu) = \int_{-\infty}^{\infty} \frac{g_{B,0}}{1 + 4\left(\frac{\nu' - (\nu_0 - \nu_B)}{\Delta\nu_B}\right)^2} S(\nu - \nu')d\nu'. \tag{8}$$

At the gain peak at $\nu = \nu_0 - \nu_B$, we get

$$\frac{G_B(\nu_0 - \nu_B)}{G_{B,0}} = \int_{-\infty}^{\infty} \frac{S((\nu_0 - \nu_B) - \nu')}{1 + 4\left(\frac{\nu' - (\nu_0 - \nu_B)}{\Delta\nu_B}\right)^2} d\nu' = \int_{-\infty}^{\infty} \frac{S(-\nu)}{1 + 4\left(\frac{\nu}{\Delta\nu_B}\right)^2} d\nu. \tag{9}$$

where the integration variable is changed according to $\nu = \nu' - (\nu_0 - \nu_B)$ and $G_{B,0}$ is the peak Brillouin gain without broadening, which is equal to $g_{B,0}$ with assumed scaling. In case of a Lorentzian optical lineshape of FWHM linewidth $\Delta\nu_{FWHM}$, Eq. (9) evaluates to $G_B/G_{B,0} = (1 + \Delta\nu_{FWHM}/\Delta\nu_B)^{-1}$, where we have dropped the frequency argument from the peak Brillouin gain (i.e., $G_B = G_B(\nu_0 - \nu_B)$). In this simple approach, the Brillouin threshold becomes proportional to $(G_B/G_{B,0})^{-1} = G_{B,0}/G_B = 1 + \Delta\nu_{FWHM}/\Delta\nu_B$. This is also equal to the enhancement in threshold, with "enhancement slope" equal to $\Delta\nu_B^{-1}$. However, this is modified for other lineshapes. For those, an "enhancement slope coefficient" k_{FWHM} can be introduced, so that $G_{B,0}/G_B = 1 + k_{FWHM}\Delta\nu_{FWHM}/\Delta\nu_B$. Note however that this is in general only an approximation to Eq. (9), valid for large optical linewidths ($\Delta\nu_{FWHM} \gg \Delta\nu_B$; the expression can then be further simplified to $G_{B,0}/G_B = k_{FWHM}\Delta\nu_{FWHM}/\Delta\nu_B$). Alternatively, one can use the RMS linewidth

Optics EXPRESS

$\Delta\nu_{RMS}$, i.e., $G_{B,0}/G_B = 1 + k_{RMS}\Delta\nu_{RMS}/\Delta\nu_B$, with a different value for the enhancement slope coefficient k_{RMS}. Table 2 summarizes the exact expressions for the integral as well as the coefficients k_{FWHM} and k_{RMS} for different optical lineshapes. Relations between the RMS and FWHM linewidths are also given. The Brillouin linewidth is still the FWHM value (the RMS linewidth of a Lorentzian spectrum is infinite). Note that the value of the slope coefficients can vary by almost a factor-of-two, depending on lineshape and linewidth definition. For $\Delta\nu_B = 45$ MHz and a Gaussian optical spectrum, the enhancement slope $k_{RMS}/\Delta\nu_B$ becomes 17.7 GHz^{-1}.

Table 2. $G_{B,0}/G_B$ from Eq. (9), k_{FWHM}, k_{RMS}, and relation between FWHM and RMS linewidth for different optical spectral shapes and a Lorentzian Brillouin spectrum.

Shape of optical spectrum S(ν)	Rectangular	Lorentzian	Gaussian
$S(\nu)$	S_{max}, $\lvert\nu\rvert<\Delta\nu_{FWHM}/2$ 0, $\lvert\nu\rvert>\Delta\nu_{FWHM}/2$	$\frac{S_{max}}{1+(\frac{2\nu}{\Delta\nu_{FWHM}})^2}$	$S_{max}e^{[-ln2(2\nu/\Delta\nu_{FWHM})^2]}$
$S_{max}\times\Delta\nu_{FWHM}$	1	$2/\pi \approx 0.6366$	$2(\ln 2/\pi)^{1/2} \approx 0.9394$
$G_{B,0}/G_B$ (Inverse of Eq. (8))	$\frac{\Delta\nu_{FWHM}/\Delta\nu_B}{\arctan\frac{\Delta\nu_{FWHM}}{\Delta\nu_B}}$	$1+\frac{\Delta\nu_{FWHM}}{\Delta\nu_B}$	$\frac{\Delta\nu_{FWHM}/\Delta\nu}{2^{(\Delta\nu_B/\Delta\nu_{FWHM})^2}\sqrt{\pi ln2}\,\mathrm{erfc}\,\frac{\Delta\nu_B\sqrt{ln2}}{\Delta\nu_{FWHM}}}$
k_{FWHM}	$2/\pi \approx 0.6366$	1	$(\pi ln2)^{-1/2} \approx 0.6777$
k_{RMS}	$2\sqrt{3}/\pi \approx 1.103$	Not applicable	$(2/\pi)^{1/2} = 0.7979$
$\Delta\nu_{RMS} = 2\sqrt{\int_{-\infty}^{\infty}\nu^2 S(\nu)d\nu}$	$3^{-1/2}\Delta\nu_{FWHM} \approx 0.5774\ \Delta\nu_{FWHM}$	Infinite	$(2ln2)^{-1/2}\Delta\nu_{FWHM} \approx 0.8493\ \Delta\nu_{FWHM}$

Funding. Ministry of Electronics and Information technology (MEITY-PHS-2693); Scheme for Promotion of Academic and Research Collaboration (SPARC/2018-2019/P942/SL); UK-India Education and Research Initiative (P942).

Disclosures. The authors declare no conflicts of interest.

Data availability. Data underlying the results presented in this paper are not publicly available at this time but may be obtained from the authors upon reasonable request.

References

1. R. Smith, "Optical power handling capacity of low loss optical ?bers as determined by stimulated Raman and Brillouin scattering," Appl. Opt. **11**(11), 2489–2494 (1972).
2. D. J. Richardson, J. Nilsson, and W. A. Clarkson, "High power fiber lasers: current status and future perspectives [invited]," J. Opt. Soc. Am. B **27**(11), B63–B92 (2010).
3. J. E. Rothenberg, P. A. Thielen, M. Wickham, and C. P. Asman, "Suppression of stimulated Brillouin scattering in single-frequency multi-kilowatt fiber amplifiers," in *Proc. SPIE 6873, Fiber Lasers V: Technology, Systems, and Applications*, vol. 687300 (2008).
4. J. Hansryd, F. Dross, M. Westlund, P. A. Andrekson, and S. N. Knudsen, "Increase of the SBS threshold in a short highly nonlinear fiber by applying a temperature distribution," J. Lightwave Technol. **19**(11), 1691–1697 (2001).
5. C. Zeringue, I. Dajani, S. Naderi, G. T. Moore, and C. Robin, "A theoretical study of transient stimulated Brillouin scattering in optical fibers seeded with phase-modulated light," Opt. Express **20**(19), 21196–21213 (2012).
6. V. R. Supradeepa, "Stimulated Brillouin scattering thresholds in optical fibers for lasers linewidth broadened with noise," Opt. Express **21**(4), 4677–4687 (2013).
7. B. Anderson, A. Flores, R. Holten, and I. Dajani, "Comparison of phase modulation schemes for coherently combined fiber amplifiers," Opt. Express **23**(21), 27046–27060 (2015).
8. C. Yu, S. Augst, S. Redmond, K. Goldizen, D. Murphy, A. Sanchez, and T. Fan, "Coherent combining of a 4 kW, eight-element fiber amplfier array," Opt. Lett. **36**(14), 2686 (2011).
9. M. Liu, Y. Yang, H. Shen, J. Zhang, X. Zou, H. Wang, L. Yuan, Y. You, G. Bai, B. He, and J. Zhou, "2.2 GHz pseudo-random binary sequence phase modulated fiber amplifier with Brillouin gain-spectrum overlap," Sci. Rep. **10**(1), 629 (2020).
10. Y. Liu, Z. Lu, Y. Dong, and Q. Li, "Research on stimulated Brillouin scattering suppression based on multi-frequency phase modulation," Chin. Opt. Lett. **7**(1), 29–31 (2009).
11. A. V. Harish and J. Nilsson, "Optimization of phase modulation with arbitrary waveform generators for optical spectral control and suppression of stimulated Brillouin scattering," Opt. Express **23**(6), 6988–6999 (2015).

Optics EXPRESS

12. J. O. White, J. T. Young, C. Wei, J. Hu, and C. R. Menyuk, "Seeding fiber amplifiers with piecewise parabolic phase modulation for high SBS thresholds and compact spectra," Opt. Express **27**(3), 2962–2974 (2019).
13. B. M. Anderson, R. Hui, A. Flores, and I. Dajani, "SBS suppression and coherence properties of a flat top optical spectrum in a high power fiber amplifier," Proc. SPIE **10083**, 100830V (2017).
14. A. V. Harish and J. Nilsson, "Optimization of phase modulation formats for suppression of stimulated Brillouin scattering in optical fibers," IEEE J. Sel. Top. Quantum Electron. **24**(3), 1–10 (2018).
15. Y. Panbiharwala, A. V. Harish, D. Venkitesh, J. Nilsson, and B. Srinivasan, "Pareto-optimized modulation formats for suppression of stimulated Brillouin scattering in optical fiber amplifiers," in *Laser Congress 2019 (ASSL, LAC, LS&C), OSA Technical Digest (Optical Society of America paper JTu3A.12*, (2019).
16. R. W. Boyd, K. Rzaewski, and P. Narum, "Noise initiation of stimulated Brillouin scattering," Phys. Rev. A **42**(9), 5514–5521 (1990).
17. Y. Wang and H. Po, "Dynamic characteristics of double-clad fiber amplifiers for high-power pulse amplification," J. Lightwave Technol. **21**(10), 2262–2270 (2003).
18. A. A. Fotiadi, P. Mégret, and M. Blondel, "Dynamics of a self-q-switched fiber laser with a Rayleigh-stimulated Brillouin scattering ring mirror," Opt. Lett. **29**(10), 1078–1080 (2004).
19. M. Hildebrandt, S. Büsche, P. Weßels, M. Frede, and D. Kracht, "Brillouin scattering spectra in high-power single frequency ytterbium doped fiber amplifiers," Opt. Express **16**(20), 15970–15979 (2008).
20. N. A. Brilliant, "Brillouin scattering spectra in high-power single frequency ytterbium doped fiber amplifiers," J. Opt. Soc. Am. B **19**(11), 2551–2557 (2002).
21. A. Liu, X. Chen, M. Li, J. Wang, D. T. Walton, and L. A. Zenteno, "Comprehensive modeling of single frequency fiber amplifiers for mitigating stimulated Brillouin scattering," J. Lightwave Technol. **27**(13), 2189–2198 (2009).
22. Y. Panbhiharwala, A. V. Harish, D. Venkitesh, J. Nilsson, and B. Srinivasan, "Investigation of temporal dynamics due to stimulated Brillouin scattering using statistical correlation in a narrow-linewidth cw high power fiber amplifier," Opt. Express **26**(25), 33409–33417 (2018).
23. Y. Censor, "Pareto optimality in multiobjective problems," Appl. Math. Optim. **4**(1), 41–59 (1977).
24. R. W. Boyd, *Nonlinear Optics* (Elsevier, 2020).
25. G. P. Agrawal, *Nonlinear Fiber Optics* (Elsevier, 2013).